

Electron paramagnetic resonance of Cu^{2+} ion pairs in $\text{CaO}:\text{Cu}$

A. Raizman, J. Barak, R. Englman, and J. T. Suss

Soreq Nuclear Research Center, Israel Atomic Energy Commission, Yavne 70600, Israel

(Received 27 March 1981)

Electron paramagnetic resonance of copper pairs was observed in $\text{CaO}:\text{Cu}$. The spectra are typical of $S = 1$ in a tetragonal symmetry with the pair axes parallel to the [100], [010], or [001] directions. The g factor is isotropic, while the hyperfine parameters are highly anisotropic. This behavior is explained by assigning the spectra to linear $\text{Cu}^{2+}-\text{O}^{2-}-\text{Cu}^{2+}$ bonds, where the two Cu ions of each pair are coupled through the bridging oxygen ion with an antiferrodistortive-ferromagnetic interaction. The ground state of the pair is composed of a θ state ($3z^2 - r^2$) of one Cu^{2+} ion and an ϵ state ($x^2 - y^2$) of the other with an exchange constant $J = -2 \text{ cm}^{-1}$.

I. INTRODUCTION

Extensive studies have been made on the electron-paramagnetic-resonance (EPR) spectra of isolated ion pairs.¹ In most of these studies the pairs consisted of similar ions and only very limited work was done on dissimilar ion pairs. Besides different ions in the pair, dissimilarity can arise from similar ions occupying sites of different symmetry² or ions with the same symmetry but with nonparallel alignment of their axes.³ An EPR spectrum of isolated ion pairs possessing an orbitally doubly degenerate ground state, such as Cu^{2+} in octahedral symmetry, has to the best of our knowledge not yet been reported by others.⁴ The aim of this work was to investigate the role that orbital degeneracy of Jahn-Teller (JT) ions plays on the superexchange interaction between the two ions of the pair, as reflected in the EPR spectrum. Other experimental techniques were used previously to study the interaction between high-density JT ions in an octahedral environment in magnetic materials. Some of these experimental results, as well as theoretical studies, were summarized by various authors.⁵⁻⁸ Kugel and Khomskii⁹ theoretically described the exchange coupling of pairs of JT impurities in a crystal. In this paper we present the interesting EPR spectrum of Cu^{2+} pairs in CaO and analyze it.

The EPR spectrum of single Cu^{2+} ions in CaO has been extensively investigated.^{10,11} It was interpreted in terms of the JT effect, in view of the doubly degenerate electronic (2E_g) ground state of Cu^{2+} in the octahedral crystal field due to the six O^{2-} ligands. The isotropic high-temperature (77 K) spectrum with $S = \frac{1}{2}$ and $g = 2.220$ consists of four lines with the typical structure of Cu^{2+} due to the two isotopes ${}^{63}\text{Cu}$ and ${}^{65}\text{Cu}$, both with $I = \frac{3}{2}$ and a small difference in the nuclear magnetic moment. The low-temperature spectrum (1.3 K) exhibited an intermediate JT effect¹¹ with $\bar{\delta}/3\Gamma \approx 0.67$, where $\bar{\delta}$ is the mean random

strain splitting of the ground vibronic doublet E and 3Γ is the tunneling splitting between the vibronic doublet and the first excited singlet A_1 or A_2 . From the angular dependence and the line shape of the EPR spectrum it was deduced that the first excited singlet of Cu^{2+} in CaO is A_1 , which means that the CuO_6 complex tends to be in a compressed configuration. However, it is usually found¹² that the Cu^{2+} ions occupy an elongated configuration. Cu^{2+} in CaO was characterized by Guha and Chase¹³ from Raman scattering measurements as a system with a strong linear and a relatively weak nonlinear JT coupling. (There is an ambiguity in the determination of the JT energy E_{JT} . These authors¹³ place E_{JT} in the range of $900-5500 \text{ cm}^{-1}$.) The value of β , the nonlinear JT coupling constant, was found experimentally to be -22.5 cm^{-1} . As long as the concentration of the Cu^{2+} impurities is small, only single-ion spectra are observed. When doping is high enough, the probability of two impurities occupying near sites is high. The interaction between the ions of such pairs gives rise to spectra which are different from those of the isolated ions and from which one can learn the structure of these pair centers.¹

The following sections give the experimental procedure, and the fine and hyperfine structures of the pair spectrum. The results are discussed and interpreted in terms of a static JT model for two neighboring Cu^{2+} ions bridged by an O^{2-} ion located between them.

II. EXPERIMENTAL RESULTS AND INTERPRETATION

A. Experimental

Copper impurities were incorporated by diffusion into CaO single crystals of 99.9% purity purchased from W. and C. Spicer Ltd. The crystals were covered with fine copper powder and heated for 4

days at 1500 °C. The faces of the crystals were cleaved mechanically after the diffusion process, to remove the excess metal. A Varian X-band spectrometer was used in the temperature range 1.7–150 K. Complementary measurements were also performed with a Varian Q-band spectrometer.

B. General description of the spectrum

A typical EPR spectrum of Cu doped CaO at 93 K and 9.079 GHz is shown in Fig. 1. The external field \vec{H} above 2000 G was along a [100]-type crystallographic direction. Below 2000 G, \vec{H} was along a [110]-type direction. The radio-frequency field \vec{H}_{rf} was perpendicular to \vec{H} in both cases. The spectrum *c* in the frame, which is attenuated by a gain of $\frac{1}{10}$, is ascribed to the Cu^{2+} single-ion transitions with an isotropic *g* factor $g_{iso} = 2.22$. The two clusters, denoted by a_{\parallel} and b_{\parallel} are identical in structure and are attributed to “ $\Delta M = \pm 1$ ” transitions (with the pair axis along the [100] direction) between energy levels of Cu^{2+} pairs with $S = 1$, as shown in Fig. 2. Each cluster exhibits a strange hyperfine structure consisting of 10 lines (instead of the expected 7 lines). This structure is discussed in Sec. IID, below. Most of the other absorption lines on both sides of the *c* spectrum belong either to tetragonal Cu^{2+} single ion sites or to magnetic ions other than Cu^{2+} . From the angular dependence of the spectrum it seems that the two

very weak clusters of lines just below the symbols a_{\perp} and b_{\perp} belong to the Cu^{2+} pairs in the [010] or [001] directions, that is, to pairs having the pair axis perpendicular to \vec{H} . Due to the cubic symmetry of the CaO matrix (NaCl structure), the same spectra (as in Fig. 1) are found if instead of $\vec{H} \parallel [100]$ we have $\vec{H} \parallel [010]$, etc.

The cluster of 10 lines denoted by “ $\Delta M = 2$ ” in Fig. 1 was taken with $\vec{H} \parallel [110]$, since it was unobservable by $\vec{H} \parallel [100]$. The integrated intensity of the pair spectrum (Fig. 1) is comparable with that of the single ion. The concentration of Cu ions in the crystal is about 1%. If a random distribution process takes place during diffusion, the concentration of ion pairs is expected to be two orders of magnitude smaller than that of the single ion. Thus it seems that, when diffused in the CaO matrix, the Cu ions prefer to occupy neighboring sites so as to form a linear $\text{Cu}^{2+}-\text{O}^{2-}-\text{Cu}^{2+}$ bond. This is further supported by the small linewidth of 7 G of the pair lines which is the same as that of the single ion in the [111] direction. This means that the pairs are well isolated from each other, as well as from the single ions. This also explains why other possible pairs, like [110] nearest-neighbor Cu^{2+} pairs, are absent from the spectrum. Another possibility is that these other pairs have a singlet ground state with too high an exchange coupling, so that the triplet level is not thermally excited.

The spectrum did not change appreciably after x-

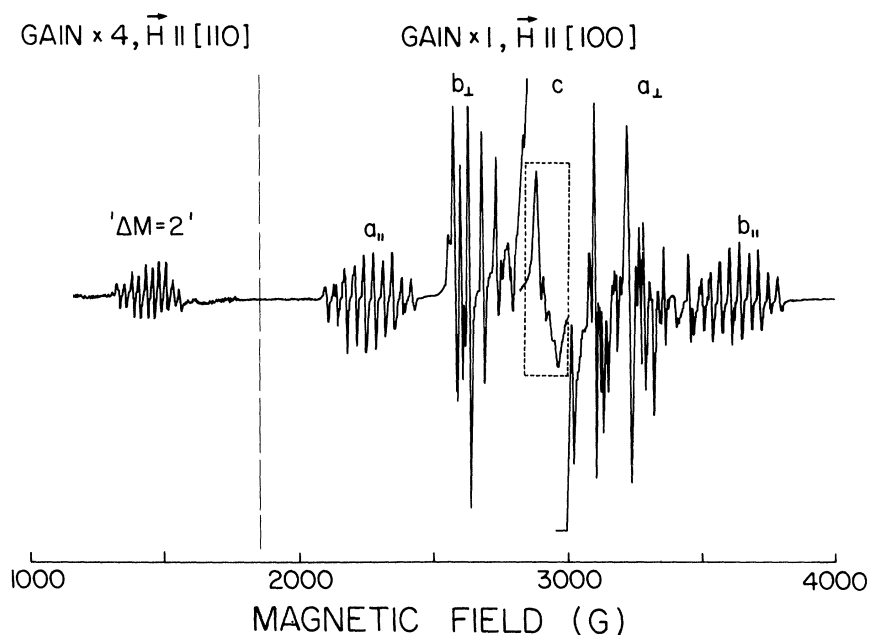


FIG. 1. The EPR spectrum of CaO:Cu at 93 K and 9.079 GHz. The spectrum in the frame (*c*) corresponds to the Cu^{2+} single ion lines for $\vec{H} \parallel [100]$ with a gain of $\frac{1}{10}$. Most of the other lines are ascribed to Cu^{2+} pairs.

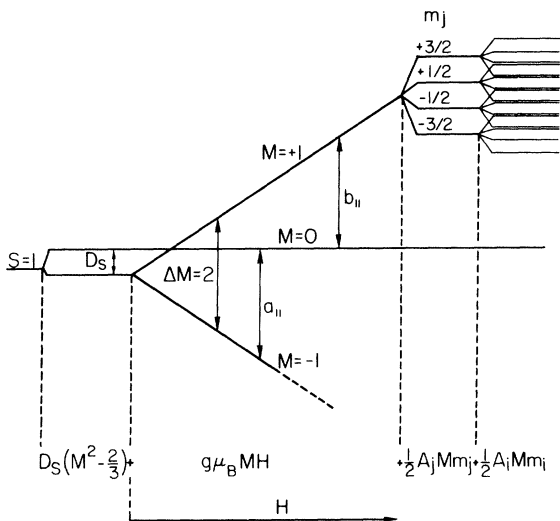


FIG. 2. The energy level diagram for the triplet state of the Cu^{2+} pair, for \vec{H} parallel to the pair axis ($\theta=0$). The fine-structure splitting with negative D_s value and the Zeeman term, along with the transitions for X-band experiments are shown. The hyperfine structure, the scale of which is enlarged by a factor of 10, is shown for the $M=1$ state. The $M=-1$ state splits in a similar way but with the m_i and m_j states in opposite order. The $M=0$ state does not split for $\theta=0$.

ray irradiation at room temperature, however after reduction in hydrogen at 1000°C the pair spectrum disappeared.

C. Fine structure

Here we refer to the center of each cluster of the fine structure of the pair spectrum. The center field between a_{\parallel} and b_{\parallel} corresponds to $g=2.21$, a value which is very close to the isotropic Cu^{2+} single ion g factor. The experimentally measured centers of the groups of lines a and b (which for $\theta=0^\circ$ are the a_{\parallel} and b_{\parallel} lines of Fig. 1) and of the " $\Delta M=2$ " clusters, are plotted (points) in Fig. 3 and are exhibited as a function of θ , the angle between \vec{H} and the [100] direction in the (001) plane. Two other clusters a_{\perp} and b_{\perp} in Fig. 1, which are unaffected by changing θ are also marked. Rotation in the (110) plane also reflects the axial symmetry of the pair spectrum. The angular behavior confirms that the observed pairs have axes parallel to the three equivalent [100]-type directions. Therefore, we will consider pairs of Cu^{2+} ions of the linear $\text{Cu}-\text{O}-\text{Cu}$ bonds in the [100], [010], and [001] directions.

Because of overlapping with the single ion spectrum, the pair spectrum could be followed over only part of the range of θ . The " $\Delta M=2$ " lines do not suffer from this limitation and their angular depen-

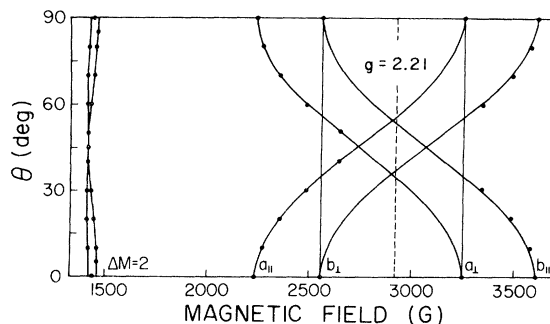


FIG. 3. The angular dependence of the fine-structure transitions of the Cu^{2+} pairs in the (001) plane. The points represent the experimental results and the solid lines show the calculated fine structure.

dence is almost complete. A detailed fine-structure angular dependence of the " $\Delta M=2$ " lines of [100] pairs is given in Fig. 4. For $\vec{H}_{\text{eff}} \perp \vec{H}$ these lines disappear at $\theta=0^\circ$ and 90° . However, for $\vec{H}_{\text{eff}} \parallel \vec{H}$ the lines were well detected at and around $\theta=90^\circ$. The angular dependence is typical of an $S=1$ spin and " $\Delta M=2$ " lines belonging to the "forbidden" $M=1 \rightarrow M=-1$ transition, as shown in Fig. 2.

We shall denote the two ions in the pair by i and j . The coupling of the two spins of the pair \vec{S}_i and \vec{S}_j , both having $S_i=S_j=\frac{1}{2}$, to a fairly pure triplet state ($S=1$) means that the exchange interaction between the two Cu^{2+} ions is large compared to the Zeeman and the fine-structure terms. We shall now write out the Hamiltonian of the pair,¹ including isotropic exchange interaction and a Zeeman term, but excluding the deformation of the lattice structure,

$$\begin{aligned} \mathcal{H} &= J\vec{S}_i \cdot \vec{S}_j + \mu_B \vec{S}_i \cdot \vec{g}_i \vec{H} + \mu_B \vec{S}_j \cdot \vec{g}_j \vec{H} \\ &= J\vec{S}_i \cdot \vec{S}_j + \frac{1}{2} \mu_B (\vec{S}_i + \vec{S}_j) \cdot (\vec{g}_i + \vec{g}_j) \vec{H} \\ &\quad + \frac{1}{2} \mu_B (\vec{S}_i - \vec{S}_j) \cdot (\vec{g}_i - \vec{g}_j) \vec{H} \end{aligned} \quad (1)$$

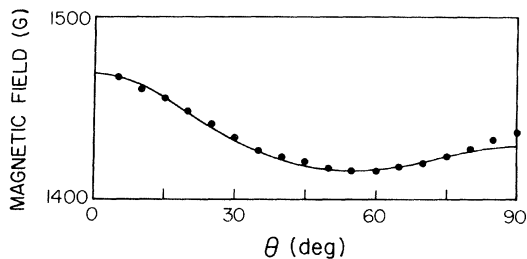


FIG. 4. Angular dependence of the fine structure of the " $\Delta M=2$ " lines for the Cu^{2+} pairs with pair axes parallel to the crystallographic [100] direction. The points represent the experimental results and the solid line shows the calculated fine structure.

where J is the isotropic exchange constant, μ_B is the Bohr magneton and \tilde{g}_i, \tilde{g}_j are the g tensors for the two ions. For a large exchange, such that

$$|J| \gg (g_i + g_j)\mu_B H, ,$$

the two spins are coupled into $\vec{S} = \vec{S}_i + \vec{S}_j$ with $S = 0$ (singlet) and $S = 1$ (triplet) states. In the case of axial symmetry, with z as the pair axis direction, the g tensors are diagonal with principal values g_{\parallel} and g_{\perp} . The last term in Eq. (1) is off diagonal in this scheme and vanishes for two identical ions, since then $\tilde{g}_i = \tilde{g}_j$.

For the axial system in its $S = 1$ state, one can write a spin Hamiltonian, adding also an electric quadrupole term,¹

$$\mathcal{H} = g_{\parallel}\mu_B H_z S_z + g_{\perp}\mu_B (H_x S_x + H_y S_y) + D_s [S_z^2 - \frac{1}{3} S(S+1)] , \quad (2)$$

where $g_{\parallel} = \frac{1}{2}(g_{\parallel}^i + g_{\parallel}^j)$, $g_{\perp} = \frac{1}{2}(g_{\perp}^i + g_{\perp}^j)$, and $D_s = 3\alpha_s D_e + \beta_s D_c$. The term D_e represents the anisotropic interaction with axial symmetry, D_c is the second-degree crystal-field term of the single ion and α_s and β_s are coefficients defined in Ref. 1. For $S_i = S_j = \frac{1}{2}$, we have $\beta_s = 0$, $D_c = 0$, and $\alpha_s = \frac{1}{2}$. $3\alpha_s D_e = D_D + D_E$, where $D_D = -3\alpha_s g_i g_j \mu_B^2 / r_{ij}^3$ is the dipolar part of the spin-spin interaction with r_{ij} the distance between the two Cu^{2+} ions. D_E is a pseudo-dipolar term which might originate from exchange anisotropy. Though the observed fine structure is highly anisotropic, the symmetry of the experimental spectrum around $g = 2.21$ (Fig. 2) surprisingly suggests an isotropic g factor for the pair. Therefore, empirically, we can simplify Eq. (2) to take the form

$$\mathcal{H} = g \mu_B \vec{S} \cdot \vec{H} + D_s [S_z^2 - \frac{1}{3} S(S+1)] \quad (3)$$

with $|D_s| = (703 \pm 5) \times 10^{-4} \text{ cm}^{-1}$. Substituting $r_{ij} = 4.9 \text{ \AA}$ into the definition of D_D , one gets $D_D = -270 \times 10^{-4} \text{ cm}^{-1}$. Thus $|D_E| > |D_D|$, as was also found for other pairs.

The Hamiltonian (3) can be written¹⁴

$$\mathcal{H} = g \mu_B S_z' H + \frac{1}{2} D_s [S_z'^2 - \frac{1}{3} S(S+1)] (3 \cos^2 \theta - 1) - D_s (S_x' S_z' + S_z' S_x') \cos \theta \sin \theta + \frac{1}{4} D_s (S_+'^2 - S_-'^2) \sin^2 \theta , \quad (4)$$

where z' is the direction of the applied field \vec{H} , θ is the angle between z' and the pair axis z , and S_z' is the spin component in the z' direction.

We used a computer program for exact diagonalization of the spin Hamiltonian (4). The calculated angular dependence of the fine structure, using the parameters in Table I, is given by solid lines in Fig. 3. For the X band the intensity of the " $\Delta M = 2$ " lines for $\vec{H}_{\text{rf}} \perp \vec{H}$ and $\theta = 45^\circ$ was calculated to be about one tenth that of the " $\Delta M = 1$ " lines (a and b) and to vanish when θ approaches 0° or 90° . This we observed experimentally. The experimental point $\theta = 90^\circ$ was obtained for $\vec{H}_{\text{rf}} \parallel \vec{H}$. The calculated angular dependence of the " $\Delta M = 2$ " transition for the [100] pair only is shown in Fig. 4. The good agreement between calculation and experiment in Figs. 2 and 3 verifies that we observe an $S = 1$ state with [100] symmetry.

The spectrum at the Q band was essentially the same, except that the " $\Delta M = 2$ " lines were not observed. Calculations show that these lines are an order of magnitude weaker in the Q band than in the X band, and could not be observed with the sensitivity of our apparatus. The distance between a_{\parallel} and b_{\parallel} lines is $2D_{\text{eff}} = 1340 \times 10^{-4} \text{ cm}^{-1}$ for the Q band. This frequency dependence of the fine-structure splitting will be discussed later (Sec. IV B).

The spectrum was investigated at different temperatures, in the range 1.7–150 K, in order to study the dependence of the various parameters on temperature. From the temperature dependence of the intensity of the EPR transitions, useful information on the magnitude of J and the sign of D_s can be obtained. A uniform increase in the intensity of the various components of the pair spectrum was observed with cooling down to 4.2 K. Below this temperature the a_{\parallel} lines become more intense than the

TABLE I. Parameters of copper-ion pairs in CaO.

| | | |
|----------------------|--------------------------|--|
| Hyperfine constants: | θ state | $A_{i\parallel} = (72 \pm 2) \times 10^{-4} \text{ cm}^{-1}$; $A_{i\perp} = (0 \pm 2) \times 10^{-4} \text{ cm}^{-1}$ |
| | ϵ state | $A_{j\parallel} = (-144 \pm 2) \times 10^{-4} \text{ cm}^{-1}$; $A_{j\perp} = (-41 \pm 2) \times 10^{-4} \text{ cm}^{-1}$ |
| | g factor: | $g = 2.21 \pm 0.005$ |
| | Exchange constant: | $J = -2.0 \text{ cm}^{-1}$ |
| | Zero-field splitting: | $D_s = (-703 \pm 5) \times 10^{-4} \text{ cm}^{-1}$ |
| | Contact term parameters: | $\kappa_{\theta} = 0.09$ |
| | | $\kappa_{\epsilon} = 0.61$ |

$b_{||}$ lines. This yields a negative sign for D_s and suggests that the $a_{||}$ lines are the transitions between the $M = -1$ and $M = 0$ levels, as shown in Fig. 2. Exact calculations even give quantitative agreement with the experimental ratio of $\frac{4}{3}$ between the intensities of the $a_{||}$ and $b_{||}$ clusters at 1.7 K. From the measured value of D_s and the calculated value of D_D one obtains $D_E \approx -430 \times 10^{-4} \text{ cm}^{-1}$. The measured D_s value was temperature independent. The average intensity of the spectrum increases by a factor of 3 on cooling from 4.2 to 1.7 K. This indicates that the isotropic exchange is either ferromagnetic or weakly antiferromagnetic with $J < 1 \text{ cm}^{-1}$. At 1.7 K the pair spectrum shows saturation effects at rf powers higher than $1 \mu\text{W}$, while the single ion spectrum is saturated at much higher power. It should be noted that at 1.7 K the Cu^{2+} single ion exhibits a quasi-static Jahn-Teller effect,¹¹ reflected by the splitting of the isotropic spectrum into two asymmetrical components, while the pair spectrum still has an isotropic g factor. The energy levels of the Cu^{2+} pair are discussed in Sec. III where these results are explained.

D. Hyperfine structure

For a pair of similar ions and a resolved hyperfine structure, each component of the structure splits into $4I + 1$ lines with a spectral weight of $1:2:3:\dots:2I + 1:\dots:3:2:1$ [a total weight of $(2I + 1)^2$]. The separation between adjacent lines is equal to half of that of the single ion.¹ When such a spectrum is observed it provides unambiguous proof that it is due to a pair center. This was the case of Cu^{2+} pairs in some matrices^{1,15} with lower than cubic symmetry and in the case of Mn^{2+} pairs in CaO .¹⁶

For a pair of identical Cu^{2+} ions with $J \gg A$, where A is the hyperfine constant, we expected, for each of the fine structure components a , b , and “ $\Delta M = 2$ ”, a hyperfine structure of 7 equally separated lines with relative intensities of $1:2:3:4:3:2:1$ [with a total weight of $(2I + 1)^2 = 16$].¹ Copper has two isotopes, ^{63}Cu and ^{65}Cu , with natural abundances of 69.09% and 30.91%, respectively, both with a nuclear spin $I = \frac{3}{2}$. The ratio of the nuclear magnetic moments of the two isotopes is $^{65}\mu_N/^{63}\mu_N = 1.071$. This should give rise to a small structure in each of the above 7 lines. For a pair of two Cu^{2+} ions in equivalent sites the mean separation between two adjacent lines at 77 K should be about $10.9 \times 10^{-4} \text{ cm}^{-1}$ which is half of the $^{63}\text{Cu}^{2+}$ single ion hyperfine constant (or about 10 G). The observed hyperfine structure is entirely different, as given in detail in Fig. 5(a) for the $a_{||}$ cluster of Fig. 1. The 10 lines have a spectral weight of $1:1:2:2:2:2:2:2:1:1$, again summing up to 16. This result indicates that the two Cu^{2+} ions of the pair are not equivalent.

The hyperfine interaction adds a term to the pair

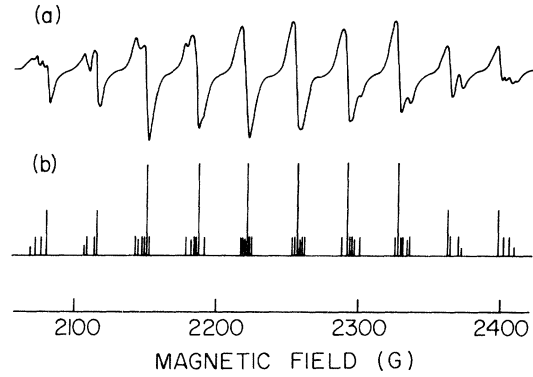


FIG. 5. (a) The detailed hyperfine structure of the $a_{||}$ lines. (b) The corresponding stick diagram with $A_j = 2A_i$ (see Fig. 2). The two copper isotopes are taken into account. This is shown by the splitting of each of the 10 lines.

Hamiltonian, Eq. (1), which for large exchange and $S_i = S_j$ takes the form¹

$$\mathfrak{H}_{\text{hf}} = \frac{1}{2} \bar{S} (\bar{A}_i \bar{I}_i + \bar{A}_j \bar{I}_j) \quad (5)$$

Here \bar{A}_i and \bar{A}_j are the hyperfine tensors of nuclei i and j , respectively, including the transferred hyperfine interaction between each of the two Cu^{2+} ions and the nucleus of the other.¹ Only one isotope of Cu^{2+} is considered for simplicity. For only small mixing between the $|M\rangle$ states which might arise, for instance, from a D_s term, Eq. (5) might be written as $\frac{1}{2} M (A_i m_i + A_j m_j)$, where m_i and m_j are the eigenvalues of I_{zi} and I_{zj} , respectively. This is the case for \bar{H} parallel to the pair axis. Transitions with $\Delta M = 1$ and $\Delta m_i = \Delta m_j = 0$ for $A_{j||} = A_{i||}$ yield the usual 7 lines of the hyperfine structure for two identical ions with $I = \frac{3}{2}$ as discussed above. If, however, $A_{j||} = 2A_{i||}$ a spectrum with 10 lines is obtained with the spectral weight described above. The right-hand part of Fig. 2 shows how the $M = \pm 1$ states split into 10 levels due to Eq. (5). Now for $\theta = 0$, the $M = 0$ state does not have a hyperfine splitting (which is not the case for $\theta \neq 0$, due to mixing between the $|M\rangle$ states as will be discussed later). Then there should be ten $|\Delta M| = 1, \Delta m_i = \Delta m_j = 0$ transitions. The exact stick diagram for this case, taking into account the possible combinations of the two Cu isotopes and their abundances, is given in Fig. 5(b) for $^{63}A_{j||} = 144 \times 10^{-4} \text{ cm}^{-1} = 2 |^{63}A_{i||}|$. The excellent agreement with the experimental results [Fig. 5(a)] confirms that the spectrum belongs to copper pairs, and to nonequivalent ions with $|A_{j||}| = 2|A_{i||}|$. (The factor 2 is precise up to some percents.) Since the “ $\Delta M = \pm 1$ ” lines could be followed only for limited values of θ , we chose to analyze the angular dependence of the hyperfine structure from the behavior of the “ $\Delta M = 2$ ” cluster. As mentioned above for \bar{H}

parallel to the pair axis ($\theta=0$), there is almost no mixing between the $|M\rangle$ states and the “ $\Delta M=2$ ” lines are not observed. For \vec{H} perpendicular to the pair axis ($\theta=90^\circ$), the Hamiltonian (4) admixes only the $|+1\rangle$ and $| -1\rangle$ states, thus with $\vec{H}_{\text{rf}} \perp \vec{H}$ the transition probability also vanishes for this direction. These lines are observable for $\theta \neq 0^\circ$, $\theta \neq 90^\circ$ with maximum intensity at $\theta \simeq 45^\circ$. The [110] direction is convenient for $\vec{H}_{\text{rf}} \perp \vec{H}$ since the two pairs with axes along the [100] and the [010] directions are equivalent ($\theta=45^\circ$) and the third pair, aligned along the [001] direction, has $\theta=90^\circ$ and thus does not show up, as explained above. The spectrum of the “ $\Delta M=2$ ” cluster in the [110] direction is given in Fig. 6(a). The structure of the 10 lines is essentially unaltered. The spectrum at $\theta=90^\circ$ was studied with $\vec{H}_{\text{rf}} \parallel \vec{H}$. The Hamiltonian in Eq. (4) shows that for this geometry there is a finite transition probability only for one kind of pairs (along the [001] direction). The spectrum is now composed of only 4 lines [Fig. 6(b)], which is possible only if one of the hyperfine constants $A_{i\perp}$ or $A_{j\perp}$ vanishes.

The angular dependence of the hyperfine structure of the “ $\Delta M=2$ ” lines is given in Fig. 7(a). Obviously A_i and A_j are highly anisotropic. Figure 7(b) shows a calculated, angle-dependent, hyperfine structure with

$$A_k^2 = (A_{k\parallel}^2 g_{\parallel}^2 \cos^2 \theta + A_{k\perp}^2 g_{\perp}^2 \sin^2 \theta) / g^2, \quad (6)$$

where $k=i,j$. Here g_{\parallel} and g_{\perp} are the components of the g factor of the pair, which in our case is isotropic,

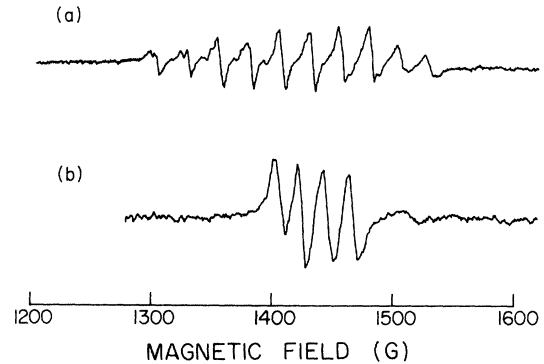


FIG. 6. The hyperfine structure of the “ $\Delta M=2$ ” lines. (a) For $\vec{H} \parallel [110]$ and $\vec{H}_{\text{rf}} \perp \vec{H}$ ($\theta=45^\circ$). (b) for $\vec{H} \perp [100]$ and $\vec{H}_{\text{rf}} \parallel \vec{H}$ ($\theta=90^\circ$).

$g_{\parallel} = g_{\perp} = g$. The hyperfine parameters which were used are given in Table I. The calculation of these values takes into account the mixing between the $|M\rangle$ states due to the D_s term, up to the second-order perturbation term (6% mixing for $\theta=90^\circ$). The agreement between the observed and calculated angular dependence is good (Fig. 7). The small differences might be due to nuclear quadrupole interactions. The angular dependence of the hyperfine splitting of the “ $\Delta M = \pm 1$ ” lines could be followed only for limited θ values up to $\theta \simeq 45^\circ$ for the a lines and up to $\theta \simeq 30^\circ$ for the b lines. The angular

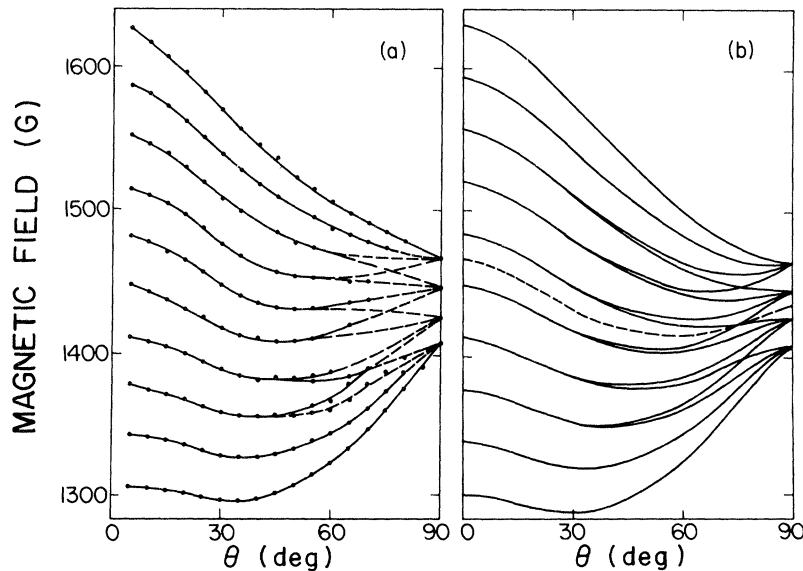


FIG. 7. The angular dependence of the “ $\Delta M=2$ ” lines. The figure shows only the lines of the pairs with axes parallel to [001]. θ is the angle of the magnetic field with respect to this direction. (a) Experimental results (the solid lines are a guide for the eye only), (b) calculated lines.

dependence shows a very peculiar behavior. The splitting of the a lines slowly increases from 34.8 G at $\theta=0^\circ$ to about 39 G at $\theta=40^\circ$ and decreases for higher θ values, while the splitting of the b lines decreases with θ much faster than that of the " $\Delta M=2$ " lines, from 34.8 G at $\theta=0^\circ$ to about 25 G at $\theta \approx 30^\circ$. However, the average of the hyperfine splitting of the a and b lines for each θ agrees well with the corresponding splitting of the " $\Delta M=2$ " lines. The different angular dependence of the hyperfine structures was explained to be due to a large amount of mixing of $|M \neq 0\rangle$ states into the $|M=0\rangle$ state, which causes, for $\theta \neq 0$, a nonzero value of $\langle M \rangle$ for the latter state.¹⁷ By numerical diagonalization of a Hamiltonian which combines Eqs. (3) and (5) we could reproduce exactly the same behavior. Thus, using the parameters in Table I, the calculated hyperfine splittings for the a and b lines as a function of θ agree with the above experimental results.

The hyperfine constants of the pair were found to be slightly temperature dependent. The splittings of A_{ij} increased by about 3.5% at 93 K as compared to 4.2 K. It should be noted that at 1.7 K, where the $\Delta m_i = \Delta m_j = 0$ lines were easily saturated, we were able to observe (unsaturated) forbidden $\Delta m \neq 0$ lines with transition probabilities much smaller than those of the $\Delta m = 0$ transitions.

III. THEORETICAL INTERPRETATION OF THE PAIR CENTER

A. Vibronic coupling

The copper pair, aligned along a [001] type direction with a bridging oxygen (the $180^\circ \text{Cu}_i^{2+}-\text{O}^{2-}-\text{Cu}_j^{2+}$ bond), forms a cluster which is shown in Fig. 8. The ground state of the Cu^{2+} single ion in the octahedral crystal field of CaO is an orbital doublet ${}^2E(t_{2g}^6 e_g^3)$, and is thus subject to a Jahn-Teller effect. It is helpful to consider the $t_{2g}^6 e_g^3$ configuration as a single hole state in the e_g^4 closed shell, with components $|\theta\rangle$ and $|\epsilon\rangle$ which transform as $(1/\sqrt{6})(2z^2 - x^2 - y^2)$ and $(1/\sqrt{2})(x^2 - y^2)$, respectively. Reynolds *et al.*¹¹ have shown that the first excited singlet of Cu^{2+} in CaO is A_1 . Thus the CuO_6 octahedron in CaO has a tendency to be compressed and to occupy the $|\theta\rangle$ vibronic state. Suppose that one Cu^{2+} ion (i) undergoes a JT effect, resulting in a $|\theta\rangle$ ground state, i.e., a compression of the O^{2-} octahedron in the z direction (where z is the pair axis). This will shorten the bond from the bridging oxygen to the i th Cu^{2+} ion while that to the j th ion will be elongated. The elongation of the oxygen octahedron surrounding the j th Cu^{2+} ion will reduce the energy of the $|\epsilon_j\rangle$ state with respect to the $|\theta_j\rangle$ state. Thus, physically, the net interaction leading to a combined

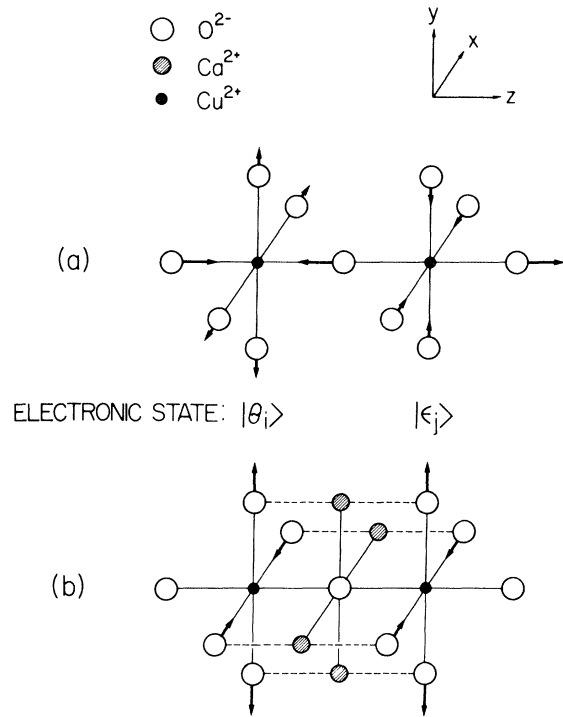


FIG. 8. The ionic cluster surrounding the copper pair. (a) The oxygen octahedron about the i copper (on the left) is compressed (arrowheaded lines), while that about the j copper is elongated. (b) The type of interaction between pairs of oxygens which gives rise to the coupling $\alpha K^2 \sigma_{\epsilon_i} \sigma_{\epsilon_j}$ is indicated by broken lines. One expects that due to this interaction both oxygens in the pair will move in the same sense (arrowheaded lines).

$|\theta_i\rangle|\epsilon_j\rangle$ ground state. It should be noted that the above argument is valid if the interaction of the pair overcomes the tendency of both CuO_6 octahedra to be in compressed configurations. We shall presently justify this for Cu in CaO.

The treatment of the pair cluster follows the analysis of the cooperative distortions in perovskites.^{6(b)} In the model given in Ref. 6(b), it is assumed that the various oxygen ions move independently of each other, i.e., that there is no oxygen-oxygen coupling. The force constant for the stretch of the bridging oxygen with respect to a copper ion is $M\omega^2$ while $M_c\omega_c^2$ represents the force constant for the relative motion of the two copper ions. Clearly the latter quantity also incorporates the resistance of the CaO lattice to compression of the cluster. The static approximation is then adopted. This amounts to neglecting the kinetic energy of the ionic motion and extremizing the vibrational potential plus electron vibration interaction, shown in Eq. (1) of Ref. 6(b). The validity of the static approximation is

based on the zero point energy being low relative to the vibronic stabilization energy or that $E_{JT}/\hbar\omega \gg 1$. Within the bounds of the estimates of Refs. 11 and 13 for CuO₆ ($E_{JT} \approx 900\text{--}6000\text{ cm}^{-1}$, $\hbar\omega = 300\text{ cm}^{-1}$), the static approximation is satisfied. We describe the ²E state in the two-dimensional orbital space (pseudospin $\frac{1}{2}$) where

$$|\theta_k\rangle = \begin{pmatrix} 1 \\ 0 \end{pmatrix}_k, \quad |\epsilon_k\rangle = \begin{pmatrix} 0 \\ 1 \end{pmatrix}_k, \quad \text{with } k = i, j. \quad (7)$$

The correlation energy between the orbital states of the two ions is^{6(b)}

$$\mathcal{K}_{\text{corr}} = K^2 \sigma_{\theta_i} \sigma_{\theta_j} \quad (8)$$

with

$$K^2 = [M_c \omega_c^2 / (M \omega^2 + 2M_c \omega_c^2)] L^2 / 12\hbar\omega. \quad (9)$$

$L (< 0)$ is a measure (with dimensions of energy), linear in the electron-vibrational coupling. The σ are the Pauli matrices

$$\sigma_{\theta} \equiv \begin{pmatrix} -1 & 0 \\ 0 & 1 \end{pmatrix}, \quad \sigma_{\epsilon} \equiv \begin{pmatrix} 0 & 1 \\ 1 & 0 \end{pmatrix} \quad (10)$$

in the orbital spaces of the centers.

Equation (8) is an appropriate expression for the tetragonal symmetry of the cluster. This symmetry also allows a term

$$\mathcal{K}'_{\text{corr}} = \alpha K^2 \sigma_{\epsilon_i} \sigma_{\epsilon_j}. \quad (8')$$

One can indeed obtain this term from a reasonable physical model (for the cluster or for its extension) by incorporating an interaction between nonbridging oxygens [Fig. 8(b)]. On the basis of the model one expects the coefficient to be negative (ferrodistortive coupling) and small compared with unity. One can then postulate wave functions on the two copper sites of the form

$$\begin{aligned} |i\rangle &= \cos\phi_i |\theta_i\rangle + \sin\phi_i |\epsilon_i\rangle, \\ |j\rangle &= \cos\phi_j |\theta_j\rangle + \sin\phi_j |\epsilon_j\rangle, \end{aligned}$$

and minimize the expectation values of the correlation Hamiltonians (8) and (8'), with respect to ϕ_i and ϕ_j . The expectation value is

$$E_{\text{corr}} = K^2 (\cos 2\phi_i \cos 2\phi_j + \alpha \sin 2\phi_i \sin 2\phi_j),$$

which is minimal for $-\alpha < 1$ at

$$\phi_i = 0, \quad \phi_j = \pi/2$$

or vice versa. The symmetry of the resulting correlated states is discussed in the Appendix.

We thus have, in the correlation Hamiltonian (8), an antiferrodistortive coupling between the two Cu²⁺ ions, meaning that the off-center displacement of the bridging oxygen favors occupation of the alternative states $|\theta\rangle$ and $|\epsilon\rangle$ by the two cations. If the nonlinear terms of the vibronic Hamiltonian represented by $|\beta|$ were large, the orbital ordering would be d_{z^2} for one center and d_{x^2} or d_{y^2} for the other, in the case of negative β (compressed octahedron).¹⁸ For positive β the corresponding orbital ordering would be $d_{x^2-y^2}$ and either $d_{z^2-y^2}$ or $d_{x^2-z^2}$ (elongated octahedron).⁹ In both cases the symmetry of the pair center would be orthorhombic rather than tetragonal. Such a lower symmetry is not consistent with the isotropic g factor and the tetragonal dependence of the hyperfine structure that were obtained in our experiments.

From Raman scattering measurements Guha and Chase¹³ found a value of -22.5 cm^{-1} for β in the CaO:Cu²⁺ system. Thus the CaO:Cu²⁺ system is one of strong linear ($E_{JT}/\hbar\omega \gg 1$) and weak nonlinear ($|\beta|/\hbar\omega \ll 1$) vibronic coupling. [Strong nonlinear coupling (with $\beta \approx 500\text{ cm}^{-1}$) occurs in some Cu²⁺ complexes, Appendix IX in Ref. 18.] To estimate the correlation energy K^2 in Eq. (8), we note that the square bracket of Eq. (9) is smaller than 1 and probably about $\frac{1}{3}$. Further, according to Refs. 11 and 19, $L^2/(12\hbar\omega) = \frac{2}{3} E_{JT} \approx 4000\text{ cm}^{-1}$, so that the interaction between the pairs, Eq. (8), is of order of 10^3 cm^{-1} and is clearly larger than $|\beta|$ which represents the tendency to discriminate between compressed and elongated configurations.

B. Superexchange coupling

The JT effect plays an important role in the magnetic interaction between the two Cu²⁺ ions. The second-order 180° superexchange interaction between state $|\theta_i\rangle$ in site i and $|\epsilon_j\rangle$ in site j via the bridging oxygen vanishes for symmetry reasons^{5,19} since the overlap integral between the p_{O_2-} orbitals on the bridging oxygen and the $|\epsilon_j\rangle$ orbital vanishes as does the direct overlap of $|\theta_i\rangle$ and $|\epsilon_j\rangle$. Only a third-order coupling through an excited state will contribute to an effective interaction between the spins \vec{S}_i and \vec{S}_j . Such an excited state is the $|\theta_j\rangle$ state of the j -th ion. Kugel and Khomskii^{8(a)} discuss this case. According to their model, an electron can only jump from $|\theta_i\rangle$ to $|\theta_j\rangle$ without changing its spin direction S_z . The superexchange Hamiltonian is then given by⁹

$$\mathcal{K}_{\text{se}} = \frac{2b^2}{U} \left\{ 2\vec{S}_i \cdot \vec{S}_j \left[\sigma_{\theta_i} \sigma_{\theta_j} \left(1 + \frac{\mathcal{J}}{U} \right) - (\sigma_{\theta_i} + \sigma_{\theta_j}) + \left(1 - \frac{\mathcal{J}}{U} \right) \right] + \frac{1}{2} \left[\sigma_{\theta_i} \sigma_{\theta_j} \left(1 + \frac{\mathcal{J}}{U} \right) + (\sigma_{\theta_i} + \sigma_{\theta_j}) \right] \right\}, \quad (11)$$

where \mathcal{J} is the exchange integral between $|\theta\rangle$ and $|\epsilon\rangle$ in the same ion. \mathcal{J} is greater than zero. U is the Coulomb interaction between these two states and b is the transfer integral for the jump $|\theta_i\rangle \rightarrow |\theta_j\rangle$, corresponding to the overlap via the bridging oxygen. Applying \mathfrak{K}_{se} to the $|\theta_i\rangle|\epsilon_j\rangle$ state, the spin-spin interaction is found to be

$$\mathfrak{K}_s = -\frac{8b^2\mathcal{J}}{U^2}\vec{S}_i\vec{S}_j,$$

which is ferromagnetic with an effective exchange constant $J = -8b^2\mathcal{J}/U^2$. It should be noted that \mathfrak{K}_{se} itself would give rise to a ferrodistorptive-antiferromagnetic ground state for the pair. It is only because of the dominance of \mathfrak{K}_{corr} that the ground state is antiferrodistorptive ferromagnetic. For this to be the case it is required that $K^2 > 12b^2/U$.

IV. DISCUSSION

A. Parameters of the spin Hamiltonian

In this section we discuss the parameters of the fine structure and hyperfine structure of the pair of Cu^{2+} ions with a $|\theta_i\rangle|\epsilon_j\rangle$ orbital ground state. The g factors and the hyperfine constants for a single Cu^{2+} ion are given by¹¹

$$g_{\parallel} = g_1 \mp 2qg_2, \quad g_{\perp} = g_1 \pm qg_2, \quad (12)$$

$$A_{\parallel} = A_1 \mp 2qA_2, \quad A_{\perp} = A_1 \pm qA_2, \quad (13)$$

where the upper sign is appropriate for $|\theta\rangle$ and the lower sign for $|\epsilon\rangle$ states. g_1 and g_2 , A_1 and A_2 are the isotropic and anisotropic parts of the g factor and the hyperfine constant, respectively. q is the Ham²⁰ reduction factor and is equal to $\frac{1}{2}$ for a strong linear JT coupling.

The second-order expressions for g_1 and g_2 (with $q = \frac{1}{2}$) may be written as²¹

$$g_1^n = g_e - 4\left(\frac{\lambda}{\Delta}\right)_n - 5\left(\frac{\lambda}{\Delta}\right)_n^2, \quad (14)$$

$$g_2^n = -4\left(\frac{\lambda}{\Delta}\right)_n - 2\left(\frac{\lambda}{\Delta}\right)_n^2,$$

where $n = \theta, \epsilon$, and $g_e = 2.0023$ is the free-electron g factor, λ is the spin-orbit coupling which is negative for an 2E hole state, and $\Delta = 10Dq$ is the cubic crystal-field splitting, as above. Covalency effects were neglected. They may be introduced through an orbital reduction factor k whose effect is only to change the ratio λ/Δ to $k\lambda/\Delta$.²¹

The g values for the pair are the average of the single ion g factors in the particular direction [Eq. (2)]. Thus $g_{\parallel}^p = \frac{1}{2}(g_{\parallel}^{\theta} + g_{\parallel}^{\epsilon})$ and $g_{\perp}^p = \frac{1}{2}(g_{\perp}^{\theta} + g_{\perp}^{\epsilon})$, where

g^p denotes the g factor of the pair.

The observed isotropic g value of the pair yields $g^p = g_{\parallel}^p = g_{\perp}^p$. This can be achieved only if the tetragonal field affects the θ and ϵ centers as a small perturbation which can be neglected. Thus $(\lambda/\Delta)_{\theta} = (\lambda/\Delta)_{\epsilon}$ and

$$g^p = g_1^n = g_e - 4\left(\frac{\lambda}{\Delta}\right)_n - 5\left(\frac{\lambda}{\Delta}\right)_n^2 \quad (n = \theta, \epsilon) \quad (15)$$

which is also the expression of the g value of the single ion in the regime of fast averaging of the JT spectrum. The experimental value of $g_{\parallel} = 2.21$ yields $(\lambda/\Delta) = -0.055$. This value is very close to that of the single ion $(\lambda/\Delta = -0.057)$. It should be noted that for a strongly coupled pair $g^p(\theta) = [(g_{\parallel}^{\theta} \cos\theta)^2 + (g_{\perp}^{\theta} \sin\theta)^2]^{1/2}$ and the fact that $g_{\parallel}^{\theta} = g_{\perp}^{\theta}$ gives rise to an isotropic $g^p(\theta)$. This means that the anisotropic g value of the two ions does not influence the pair spectra even for $\theta \neq 0^\circ, 90^\circ$.

The hyperfine constants A_1 and A_2 are given by²¹

$$A_1^n = -P\left[\kappa_n + 4\frac{\lambda}{\Delta}\right], \quad A_2^n = -P\left[\frac{4}{7} + \frac{34}{7}\frac{\lambda}{\Delta}\right] \quad (n = \theta, \epsilon). \quad (16)$$

Here $P = 2\gamma_N\mu_B\mu_N\langle r^{-3} \rangle$, where γ_N and μ_N are the nuclear gyromagnetic (magnetogyric) ratio and the nuclear magneton, respectively. $\langle r^{-3} \rangle$ is the one electron average of r^{-3} and κ is the core polarization factor characterizing the contact hyperfine interaction. We used the same value of P for both $|\theta_i\rangle$ and $|\epsilon_j\rangle$. Though there is no experimental proof that the radial average $\langle r^{-3} \rangle$ is the same for both states, this type of average is the one that makes up the spin-orbit-coupling coefficient λ , which is equal for both states since, as mentioned above, we have an isotropic g factor for the pair spectrum. Since A_2 depends only on P and λ/Δ , we conclude that $A_2^{\epsilon} = A_2^{\theta}$. To be consistent with Eq. (13), we choose negative signs for both A_{\parallel}^{ϵ} and A_{\perp}^{ϵ} and a positive sign for A_{\parallel}^{θ} . Substituting the value $\lambda/\Delta = -0.055$ and the measured hyperfine constants from Table I into Eqs. (13) and (16), one gets $A_2^{\epsilon} = -68 \times 10^{-4} \text{ cm}^{-1}$ and $A_2^{\theta} = -48 \times 10^{-4} \text{ cm}^{-1}$. Taking the mean value $-58 \times 10^{-4} \text{ cm}^{-1}$ of A_2^{ϵ} and A_2^{θ} , we get $P = 190 \times 10^{-4} \text{ cm}^{-1}$, which corresponds to $\langle r^{-3} \rangle = 4.32 \text{ a.u.}$ Substituting the value of P into A_1^n of Eq. (16) yields $\kappa_{\theta} \approx 0.09$ and $\kappa_{\epsilon} \approx 0.61$.

In most cases the Cu^{2+} ion occupies the $|\epsilon\rangle$ state. Negative signs for A_{\parallel}^{ϵ} and A_{\perp}^{ϵ} were assumed by many authors.²² Reynolds *et al.*¹¹ obtained (for $q = \frac{1}{2}$) $A_{\parallel}^{\theta} = \pm 79 \times 10^{-4} \text{ cm}^{-1}$ and $A_{\perp}^{\theta} = \pm 7 \times 10^{-4} \text{ cm}^{-1}$ for Cu^{2+} single ions in CaO which occupy mainly the $|\theta\rangle$ state. These results are in good agreement with our results for A^{θ} . The proposed value of P is

compatible with the range $(130-360) \times 10^{-4} \text{ cm}^{-1}$ obtained for Cu^{2+} in some other hosts.¹² Hartree-Fock calculations for the free Cu^{2+} ion give a value of $390 \times 10^{-4} \text{ cm}^{-1}$.²³ A value of $\kappa_\theta \approx 0.002$ was obtained for Cu^{2+} in CaO ,¹¹ while for κ_ϵ in MgO a value of ≈ 0.3 was obtained.¹² Our estimate for $\kappa_\epsilon(0.61)$ is somewhat larger than these obtained in the literature. However, the net spin density $\chi = -\frac{3}{2}\kappa\langle r^{-3} \rangle \approx -4$ a.u. is very close to that reported in the literature.²²

The great difference between κ_θ and κ_ϵ can not be explained within our model by the tetragonal symmetry, since this should lead to nonequal values of λ/Δ and A_2 for the two states. However, a different extent of admixing by the oxygen $4s$ wave function into $|\theta_i\rangle$ and $|\epsilon_j\rangle$ ground states, which gives a positive contribution to the net spin density on the nuclei, may be the source of the difference in κ_θ and κ_ϵ .

It should be noted that the ratio $|A_{\parallel}^{\epsilon}/A_{\parallel}^{\theta}| = 2$, shown in Sec. IID seems to be accidental.

B. Exchange interaction

The rigid-lattice Hamiltonian of the isotropic exchange interaction between the spins of the pair was given in Eq. (1). In the level scheme of $|SM\rangle$ and for diagonal g tensors this Hamiltonian has off-diagonal terms only between the $M=0$ states. The matrix for the $|00\rangle$ and $|10\rangle$ levels is given by

$$\begin{aligned} |00\rangle: & \begin{pmatrix} -\frac{3}{4}J & \frac{\Delta g}{2}\mu_B H \\ \frac{\Delta g}{2}\mu_B H & \frac{1}{4}J \end{pmatrix}, \\ |10\rangle: & \end{pmatrix}, \end{aligned} \quad (17)$$

where $\Delta g \equiv g_i - g_j$ which is equal to $2g_2 = 0.43$ for $\theta = 0$. Suppose that J is negative (ferromagnetic coupling) so that $|00\rangle$ is higher in energy. $|10\rangle$ is thus pushed down, relative to $|1 \pm 1\rangle$, by

$$\Delta E = -\frac{1}{2} \{J + [J^2 + (\Delta g \mu_B H)^2]^{1/2}\} + J. \quad (18)$$

Since $D_s < 0$ and $\theta = 0$ (Fig. 2), this has the effect of reducing the fine structure splitting which is due to the D_s term (within $|\Delta M| = 1$ transitions). In second-order perturbation the effect is proportional to H^2 . Experimentally in the higher-field measurements (Q band) the splitting was smaller than for the lower fields (X band). This implies directly that J and D_s have the same sign, or since $D_s < 0$, we find that $J < 0$. Only this combination of signs is compatible with our results.

Besides determining its sign, it is also possible to calculate the value of J on the basis of the experimental results. The effective fine structure splitting for $\theta = 0$ is $2D_{\text{eff}}^X = 1406 \times 10^{-4} \text{ cm}^{-1}$ for the X -band measurements with $H \approx 3000 \text{ G}$ compared with $2D_{\text{eff}}^Q = 1340 \times 10^{-4} \text{ cm}^{-1}$ for the Q -band measure-

ments with $H \approx 10600 \text{ G}$. $D_{\text{eff}}^X - D_{\text{eff}}^Q$ corresponds to the variation in ΔE according to Eq. (18) with the change in H when going from X band to Q band. With $\Delta g = g_{\parallel} - g_{\perp} = 0.43$ and $g = 2.21$ we obtain $J \approx -2.0 \text{ cm}^{-1}$. This is the exchange constant when both \vec{S}_i and \vec{S}_j are parallel to the pair direction. The exchange might also have an anisotropic part²⁴ which gives rise to the term D_E , discussed in Sec. II. Its value is about 0.04 cm^{-1} . Evidently, this is rather small.

Since the matrix (17) admixes the $|10\rangle$ state into the $|00\rangle$ state it should be possible to observe the "forbidden transition $\Delta S = 0$ " between, for instance, $|00\rangle$ and $|11\rangle$ states. With the above value of J these transitions are expected at about $H = 17000 \text{ G}$ for $\theta = 0$ and X -band frequencies, with good intensity at 4.2 K .

Substituting the values of $J = -2 \text{ cm}^{-1}$, $U = 4.7 \times 10^4 \text{ cm}^{-1}$ (Ref. 19) and $\mathcal{J} = 8 \times 10^3 \text{ cm}^{-1}$ into $J = -8b^2\mathcal{J}/U^2$ one gets $|b| \approx 260 \text{ cm}^{-1}$. This value is much smaller than the value $b = 1500 \text{ cm}^{-1}$, obtained from the approximation¹⁹ $b \approx \Delta/6$ for $|\theta_i\rangle - |\theta_j\rangle$ overlapping in the case of antiferromagnetic coupling between the two spins.

The inequality at the end of Sec. III, giving the criterion for the dominance of the vibronic over the superexchange coupling, can be directly estimated from the above expression for J . The right-hand side of the inequality, $12b^2/U$, is then about 20 cm^{-1} , which is clearly smaller than our estimate for $K^2 (\approx 10^3 \text{ cm}^{-1})$, based on $E_{JT} = 6000 \text{ cm}^{-1}$ and also smaller than more cautious estimates arising from lower values of the Jahn-Teller energy.¹³ On the other hand, the substitution of the value 1500 cm^{-1} for b would raise the right-hand side of the inequality to 600 cm^{-1} . The effect that matrix (17) has on the angular dependence of the fine structure (Figs. 3 and 4) is rather small (less than 2 G for the X -band, and less than 8 G for the Q -band experiments) and could not be observed.

V. CONCLUSION

The introduction of a high concentration of copper ions into the CaO matrix led to the study of the interaction between Jahn-Teller ions. The EPR spectra of these ions were clear and could be precisely parametrized in order to analyze the ground state of such Jahn-Teller pairs.

Besides the single-ion line we received high-intensity triplet spectra which implies that we observed Cu^{2+} pairs coupled to $S = 1$. The angular dependence of the spectra shows tetragonal symmetry with the axial direction parallel to one of the equivalent $[100]$ cubic directions. If we consider the nearest sites that have this symmetry, we find that the observed pairs are next nearest neighbors forming linear $\text{Cu}^{2+}-\text{O}^{2-}-\text{Cu}^{2+}$ bonds. From the narrow

linewidth of the pair spectra, from their high intensity compared with the single ion line and the absence of lines of other types of pairs, we conclude that the Cu^{2+} ions in CaO prefer clustering with these linear bonds. Comparable concentrations of other types of pairs would be observable with our apparatus, if they had a ferromagnetic exchange interaction or (in the upper ranges of the temperatures) if they had an antiferromagnetic coupling with $J \leq 500 \text{ cm}^{-1}$. We could not observe any such other pairs. This indicates that due to the diffusion for long time at high temperatures (1500°C , $kT = 1230 \text{ cm}^{-1}$) the ions are trapped in clusters with high $E_{JT} (\approx 6000 \text{ cm}^{-1})$.

The value of the fine-structure splitting D_s of the observed pairs is about two and a half times larger than the one calculated for the dipolar interaction. This might arise from an anisotropic exchange coupling. The sign of D_s was found to be negative as expected for the dipolar interaction.

From the difference between the fine-structure splitting in the X -band and Q -band measurements and from the temperature dependence of the intensity of the spectra, one deduces that the pairs are ferromagnetically coupled with $J \approx -2.0 \text{ cm}^{-1}$, while the usual 180° superexchange coupling between similar ions is expected to be antiferromagnetic.

The hyperfine structure spectra show splitting due to the two copper isotopes, confirming that the spectra are indeed from Cu^{2+} pairs. However, they are highly anisotropic (with tetragonal symmetry) and do not have the structure of pairs of similar ions. It is thus concluded that the ions of the pair have different ground states. Analyzing all possible states for the $\text{Cu}^{2+}-\text{O}^{2-}-\text{Cu}^{2+}$ cluster, in view of the tetragonal symmetry of the spectra and the observed isotropic g factor, we found that the two copper ions are subject to vibronic coupling leading to a strong antiferrodistortive interaction along the pair axis. This gives rise to a ground state of the pair which consists of a static $|\theta\rangle$ on one ion and an $|\epsilon\rangle$ on the other. This interaction contributes to the preference, noted above, of the Cu^{2+} ions to form linear pair clusters.

The basic causes for the observed situation are the electronic degeneracy in the individual copper ions, the strong, or moderately strong, linear Jahn-Teller interaction (E_{JT}) and the weak anisotropic coupling (β) which tolerates the domination of the pair interaction (antiferrodistortive). It would be interesting to observe pairs in other systems with similar characteristics.

ACKNOWLEDGMENTS

We thank Professor Z. Luz for the use of his Q -band spectrometer and Dr. R. Poupko and Ms. N. Schwartz for experimental assistance.

APPENDIX A: STRUCTURE OF THE ORBITAL-VIBRATIONAL GROUND STATE

In Sec. III A we argued that vibronic coupling favors a pair configuration in which the two copper ions occupy different states of the degenerate level. The structure of the ground-state solution will now be shown to depend on a potential V_{ov} in the region of overlap between the right and left displaced position of the bridging oxygen, on the random strain e_u of odd symmetry locally differentiating between the two copper sites and on V_u the corresponding strain coupling coefficient. If the two sites are fully equivalent then, in the notation of Sec. III A, the orbit-vibrational states will have the even-odd (e/o) form

$$\psi_{e/o} = f(Z - Z_0)|\theta_i\rangle|\epsilon_j\rangle \pm f(Z + Z_0)|\epsilon_i\rangle|\theta_j\rangle \quad (A1)$$

Here Z is the coordinate of the bridging oxygen with respect to its motion between the cations, f is the wave function describing the motion relative to the equilibrium positions $\pm Z_0 = \pm |K|(2/M\omega^2)^{1/2}$. In the static approximation f^2 is a delta function. The sign in Eq. (A1) corresponding to the ground state will depend on the overlap potential V_{ov} .

If, however, there is an odd-symmetry local strain e_u , such that

$$\Theta V_{ov} \ll V_u e_u \quad (A2)$$

one or the other of the terms in Eq. (A1) will be the ground state. (This is the static limit or the frozen-in configuration.) The overlap

$$\Theta = \int f(Z - Z_0)f(Z + Z_0)dZ$$

and the effective potential V_{ov} in the overlap region which mixes the electronic states in the two parts of Eq. (A1) appear in Eq. (A2). Physically the interelectronic Coulomb interaction or exchange can cause mixing. In practice the right-hand side of (A2) is of the order of 1 cm^{-1} and for strong coupling ($K^2/\hbar\omega \gg 1$) the inequality is likely to hold, although it is not easily estimated. If the two members of (A2) are comparable, the wave function is not simple. Even so, the considerations in the text are probably unchanged, as regards the interpretation of the EPR spectrum. This follows since the two parts of (A1) are only coupled by a two-electron operator.

- ¹J. Owen and E. A. Harris, in *Electron Paramagnetic Resonance*, edited by S. Geschwind (Plenum, New York, 1972), Chap. 6.
- ²J. W. Culvahouse and D. P. Schinke, *Phys. Rev.* **187**, 671 (1969).
- ³S. G. Carr, T. D. Smith, and J. R. Pilbrow, *J. Chem. Soc. Faraday Trans. 2* **70**, 497 (1974).
- ⁴A preliminary report was given in J. Barak, R. Englman, A. Raizman, and J. T. Suss, *Solid State Commun.* **37**, 685 (1981).
- ⁵J. B. Goodenough, *Magnetism and the Chemical Bond* (Interscience, New York, 1963).
- ⁶(a) R. Englman and B. Halperin, *Phys. Rev. B* **2**, 75 (1970); (b) B. Halperin and R. Englman, *ibid.* **3**, 1698 (1971).
- ⁷M. V. Eremin and V. N. Kalinenkov, *Fiz. Tverd. Tela (Leningrad)* **20**, 3546 (1978) [*Sov. Phys. Solid State* **20**, 2051 (1978)].
- ⁸(a) K. I. Kugel and D. I. Khomskii, *Zh. Eksp. Teor. Fiz.* **64**, 1429 (1973) [*Sov. Phys. JETP* **37**, 725 (1973)]; (b) D. I. Khomskii and K. I. Kugel, *Solid State Commun.* **13**, 763 (1973).
- ⁹K. I. Kugel and D. I. Khomskii, *Fiz. Tverd. Tela (Leningrad)* **15**, 2230 (1973) [*Sov. Phys. Solid State* **15**, 1490 (1974)].
- ¹⁰W. Low and J. T. Suss, *Phys. Lett.* **7**, 310 (1963).
- ¹¹R. W. Reynolds, L. A. Boatner, M. M. Abraham, and Y. Chen, *Phys. Rev. B* **10**, 3802 (1974).
- ¹²Robert E. Coffman, *J. Chem. Phys.* **48**, 609 (1968).
- ¹³S. Guha and L. L. Chase, *Phys. Rev. B* **12**, 1658 (1975).
- ¹⁴A. Abragam and B. Bleaney, *Electron Paramagnetic Resonance of Transition Ions* (Oxford University Press, Oxford, 1970), p. 157.
- ¹⁵C. V. Manjunath and R. Srinivasan, *J. Magn. Reson.* **28**, 177 (1977).
- ¹⁶E. A. Harris, *J. Phys. C* **5**, 338 (1972).
- ¹⁷M. Decorps and F. Genoud, *J. Magn. Reson.* **35**, 247 (1979).
- ¹⁸R. Englman, *The Jahn-Teller Effect in Molecules and Crystals* (Wiley, New York, 1972), p. 36.
- ¹⁹P. W. Anderson, *Phys. Rev.* **115**, 2 (1959).
- ²⁰F. S. Ham, in *Electron Paramagnetic Resonance*, edited by S. Geschwind (Plenum, New York, 1972), p. 1.
- ²¹L. A. Boatner, R. W. Reynolds, Y. Chen, and M. M. Abraham, *Phys. Rev. B* **16**, 86 (1977).
- ²²R. R. McGarvey, *J. Phys. Chem.* **71**, 51 (1967).
- ²³J. A. C. McMillan and T. Halpern, *J. Chem. Phys.* **55**, 33 (1971).
- ²⁴D. I. Khomskii and K. I. Kugel, *Solid State Commun.* **35**, 409 (1980).